

# DEFLECTION OF MULTILAYER-SANDWICH BEAMS WITH APPLICATION TO PLYWOOD PANELS<sup>1</sup>

*R. O. Foschi*

Department of the Environment, Canadian Forestry Service  
Western Forest Products Laboratory, Vancouver, British Columbia

(Received 24 May 1973)

## ABSTRACT

The deflection of multilayer-sandwich beams (or plates with a dominant dimension in plan) when all layers are weak in shear is studied with a finite-element approach. The theory is applied to the deflection of plywood when soaked (moisture content more than 30%), and a particular case of five-ply plywood is studied in detail. The numerical results are shown to converge rapidly with increasing number of elements and the theoretical predictions are verified by experimental measurements. It is shown that the influence of shear deformations on the deflection of plywood, when soaked, is important and should be taken into account in design specifications.

*Additional keywords:* sandwich plates, plywood, finite elements, concrete forms, structural engineering.

## INTRODUCTION

Conventional sandwich plates with two stiff face layers and a weak core have been extensively investigated (Plantema 1966) and, more recently, multilayer plates with  $n$  stiff layers and  $n-1$  weak cores have received attention from several researchers. A triangular finite element for the bending analysis of such plates has recently been published (Khatua and Cheung 1972) and other authors have analyzed the problem using series solutions (Azar 1968). In all these studies, however, the strain energy due to shear deformations is calculated for the weak cores and neglected for the stiff layers.

There are cases in which this assumption cannot be made. Consider, for example, the case of plywood when the grain in the stiff face layers is parallel to the span and the grain in the weak cores perpendicular to it. The shear modulus for the stiff layers is the longitudinal-radial  $G_{LR}$  of the wood, while that for the weak cores is the radial-tangential  $G_{RT}$  of the wood. The latter is several times smaller than the former and

both show a marked decrease with an increase in moisture content. When the plywood is completely soaked, with moisture content more than 30% (case of concrete forms, for example), both moduli are relatively small and shear deformations cannot be neglected in any layer. Chiu and Biblis (1971) presented a method of computation for shear deflections in plywood. Their simplified approach, however, does not satisfy interply continuity of shear stresses. This paper presents a finite-element approach to the problem of deflections in multilayer-sandwich beams (or plates with a dominant dimension in plan) when all the shear deformations have to be accounted for.

## GENERAL THEORY

### *Assumptions*

1. The weak cores are assumed to provide resistance to shear deformation only.
2. There is no normal strain in the direction perpendicular to the span of the beam and, therefore, all points on the same perpendicular have the same vertical displacement.
3. Both the normal and shear strains are considered in the calculation of the strain energy contribution of the stiff layers.
4. The position of the neutral axis is

<sup>1</sup>The experimental data presented herein were made available through the cooperation of the Research and Development Laboratory, Council of Forest Industries of British Columbia, North Vancouver, Canada.

assumed known because of symmetry of construction of the plate. This plane is used as the origin  $z = 0$  to refer the position of the different layers.

#### Deformations and strain energy

Consider Fig. 1. The  $n$ th layer has a thickness  $t_n$  and it is located at a distance  $z_n$  from the neutral axis  $z = 0$ . After deformation, points A, B, and C will be located at A', B', and C'. The displacement  $u$  in the  $x$  direction for an arbitrary point C in this layer can be expressed as

$$u = -z \frac{dw}{dx} + u; \quad (1)$$

while, according to assumption 2, the vertical displacement of C is the common deflection  $w$ . The shear strain  $\gamma$  at C is then given by

$$\begin{aligned} \gamma &= \frac{\partial u}{\partial z} + \frac{\partial w}{\partial x} = -\frac{dw}{dx} + \\ \frac{\partial u'}{\partial z} + \frac{dw}{dx} &= \frac{\partial u'}{\partial z} \end{aligned} \quad (2)$$

and the increment  $\delta u^*$  in the displacement  $u^*$  between points A' and C' is, therefore,

$$\delta u'(z) = \int_{z_n}^z \gamma dz. \quad (3)$$

It is convenient to change variables from  $z$  to  $\eta$  according to

$$z = z_n + (1 + \eta) \frac{t_n}{2} \quad (4)$$

and Eq. 3 can thus be expressed as

$$\delta u'(\eta) = \frac{t_n}{2} \int_{-1}^{\eta} \gamma d\eta. \quad (5)$$

The shear strain  $\gamma$  is constant in the weak cores, as implied by assumption 1. On the other hand, the shear strain in the stiff layers varies with  $\eta$  and in a first approximation this variation can be assumed to be quadratic. A parabolic shear distribution is the result of the first-order approximation made in the ordinary theory of bending of beams and plates. It is assumed, therefore, that, in general,

$$\gamma(\eta) = \gamma_n + a\eta + b\eta^2 \quad (6)$$

where  $\gamma_n$  is then the shear strain at the center of the layer.

When the layer is a weak core, the shear strain is simply given by

$$\gamma(\eta) = \gamma_n. \quad (7)$$

When the  $n$ th layer is stiff, the neighboring layers are weak cores with constant shear strain, and continuity of shear stresses at the interfaces between these layers provides two equations for the determination of the constants  $a$  and  $b$  in Eq. 6. Thus, for a stiff layer

$$\begin{aligned} \gamma(\eta) &= \left( \frac{G_{n-1}}{G_n} \right) (\eta-1) \frac{\eta}{2} \gamma_{n-1} + \\ (1-\eta^2) \gamma_n &+ \left( \frac{G_{n+1}}{G_n} \right) (\eta+1) \frac{\eta}{2} \gamma_{n+1} \end{aligned} \quad (8)$$

where  $G_n$  is the shear modulus corresponding to the  $n$ th layer.

Assume now that the  $n$ th layer is stiff. Introducing Eq. 8 into Eq. 5 and integrating,

$$\begin{aligned} \delta u'(\eta) &= \left( \frac{G_{n-1}}{G_n} \right) \frac{t_n}{2} \left( \frac{\eta^3}{6} - \frac{\eta^2}{4} + \right. \\ \frac{5}{12} \gamma_{n-1} &+ \frac{t_n}{2} \left( \eta - \frac{\eta^3}{3} + \frac{2}{3} \right) \gamma_n + \\ \left. \left( \frac{G_{n+1}}{G_n} \right) \frac{t_n}{2} \left( \frac{\eta^2}{4} + \frac{\eta^3}{6} - \frac{1}{12} \right) \gamma_{n+1}. \right. \end{aligned} \quad (9)$$

The total increment in  $u^*$  due to shear deformation of the  $n$ th stiff layer is obtained for  $\eta = 1$  in Eq. 9, that is

$$\begin{aligned} (\Delta u')_n &= \left( \frac{G_{n-1}}{G_n} \right) \frac{t_n}{6} \gamma_{n-1} + \\ \frac{2}{3} t_n \gamma_n &+ \left( \frac{G_{n+1}}{G_n} \right) \frac{t_n}{6} \gamma_{n+1}. \end{aligned} \quad (10)$$

Introducing now Eq. 7 into Eq. 5 and letting  $\eta = 1$ , the total increment in  $u^*$  due to the shear deformation of a weak core is

$$(\Delta u')_n = t_n \gamma_n. \quad (11)$$

Assume once again that the  $n$ th layer is stiff. The total displacement  $u$  for an arbitrary point C in this layer is given by Eq. 1.

The displacement  $u^*$  for C can be obtained as the sum of the contributions from all the stiff and weak layers between the  $n$ th and the neutral axis according to Eqs. 10 and 11, respectively. Furthermore, the increment in  $u^*$  due to the deformation of the  $n$ th layer itself, as given by Eq. 9, must be added. That is,

$$\begin{aligned}
 u_n = & -z \frac{dw}{dx} + \sum_{i=1}^{n-1} t_i \gamma_i \theta_w(i) + \\
 & \sum_{i=1}^{n-1} \left\{ \left( \frac{G_{i-1}}{G_i} \right) \frac{t_i}{6} \gamma_{i-1} + \frac{2}{3} t_i \gamma_i + \right. \\
 & \left. \left( \frac{G_{i+1}}{G_i} \right) \frac{t_i}{6} \gamma_{i+1} \right\} \theta_s(i) + \\
 & \left( \frac{G_{n-1}}{G_n} \right) \frac{t_n}{2} \left( \frac{\eta^3}{6} - \frac{\eta^2}{4} + \frac{5}{12} \right) \gamma_{n-1} + \\
 & \frac{t_n}{2} \left( \eta - \frac{\eta^3}{3} + \frac{2}{3} \right) \gamma_n + \\
 & \left( \frac{G_{n+1}}{G_n} \right) \frac{t_n}{2} \left( \frac{\eta^2}{4} + \frac{\eta^3}{6} - \frac{1}{12} \right) \gamma_{n+1}
 \end{aligned} \quad (12)$$

where the functions  $\theta_w(i)$  and  $\theta_s(i)$  are defined such that:

for a weak layer,  $\theta_w(i) = 1$  and  $\theta_s(i) = 0$ ;

for a stiff layer,  $\theta_w(i) = 0$  and  $\theta_s(i) = 1$ .

The normal strain  $\epsilon_n$  in the  $n$ th layer can now be calculated from

$$\epsilon_n = \frac{\partial u_n}{\partial x} \quad (13)$$

giving, from Eq. 12,

$$\begin{aligned}
 \epsilon_n = & -z w'' + \sum_{i=1}^{n-1} t_i \gamma_i' \theta_w(i) + \\
 & \sum_{i=1}^{n-1} \left\{ \left( \frac{G_{i-1}}{G_i} \right) \frac{t_i}{6} \gamma_{i-1}' + \frac{2}{3} t_i \gamma_i' + \right. \\
 & \left. \left( \frac{G_{i+1}}{G_i} \right) \frac{t_i}{6} \gamma_{i+1}' \right\} \theta_s(i) + \\
 & \left( \frac{G_{n-1}}{G_n} \right) \frac{t_n}{2} \left( \frac{\eta^3}{6} - \frac{\eta^2}{4} + \frac{5}{12} \right) \gamma_{n-1}' + \\
 & \frac{t_n}{2} \left( \eta - \frac{\eta^3}{3} + \frac{2}{3} \right) \gamma_n' + \\
 & \left( \frac{G_{n+1}}{G_n} \right) \frac{t_n}{2} \left( \frac{\eta^2}{4} + \frac{\eta^3}{6} - \frac{1}{12} \right) \gamma_{n+1}' .
 \end{aligned} \quad (14)$$

If  $E_n$  and  $G_n$  are, respectively, the elastic

moduli for normal and shear strains for the  $n$ th stiff layer, its strain energy per unit width is given by

$$U_n = \int_0^L \left\{ \frac{E_n t_n}{4} \int_{-1}^1 \epsilon_n^2 d\eta + \frac{G_n t_n}{4} \int_{-1}^1 \gamma^2 d\eta \right\} dx \quad (15)$$

where  $L$  is the span of the beam or plate, the normal strain  $\epsilon_n$  is given by Eq. 14 and the shear strain  $\gamma$  by Eq. 8.

For a weak core and according to assumption 1, the strain energy is due to shear deformation only. Therefore, from Eq. 7,

$$U_n = \int_0^L \frac{G_n t_n}{2} \gamma_n^2 dx \quad (16)$$

The total strain energy  $U$ , per unit width of beam or plate, is given by the sum of the contributions from individual layers according to Eq. 15 or Eq. 16, depending on whether the layer is stiff or weak.

Consider a particular case as shown in Fig. 2. Layers 1 and 3 are assumed to be stiff while layer 2 is the weak core;  $t_1$ ,  $t_2$  and  $t_3$  are the corresponding thickness and  $E_1$ ,  $E_3$ ,  $G_1$ ,  $G_2$  and  $G_3$  are, respectively, the corresponding elastic and shear moduli. The construction is assumed balanced, and the neutral axis is thus located on the mid-plane of the panel. Equations 15 and 16 can be used to obtain the expression for the strain energy  $U$ . The calculations are tedious, if straightforward, and only the final result is presented here. The total energy can be expressed as follows,

$$\begin{aligned}
 U = \int_0^L \left\{ Q_1 (w'')^2 + Q_2 w'' \gamma_1' + \right. \\
 Q_3 w'' \gamma_2' + Q_4 w'' \gamma_3' + Q_5 (\gamma_1')^2 + \\
 Q_6 (\gamma_2')^2 + Q_7 (\gamma_3')^2 + Q_8 \gamma_1' \gamma_2' + \\
 Q_9 \gamma_1' \gamma_3' + Q_{10} \gamma_2' \gamma_3' + Q_{11} (\gamma_1')^2 + \\
 Q_{12} (\gamma_2')^2 + Q_{13} (\gamma_3')^2 + Q_{14} \gamma_1' \gamma_2' + \\
 \left. Q_{15} \gamma_2' \gamma_3' \right\} dx ;
 \end{aligned} \quad (17)$$

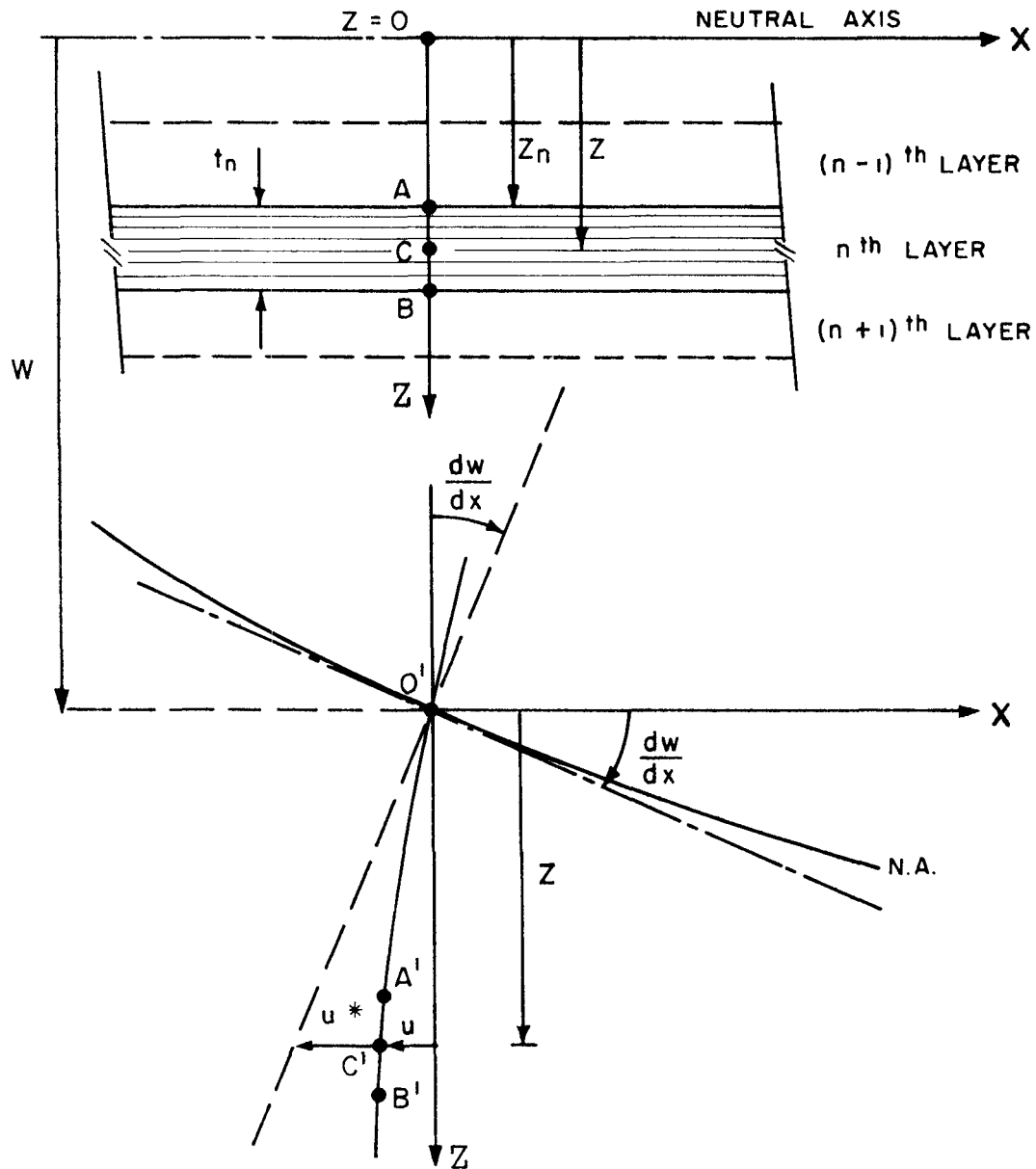


FIG. 1. Deformation of the layered system.

where the constants  $Q_i$  are given in Appendix I.

FINITE-ELEMENT ANALYSIS

As shown in Eq. 17, the strain energy expression contains the second derivative of the deflection  $w$  and first derivatives of the shear strains. A finite-element dis-

cretization must satisfy, for convergence, continuity in both functions and first derivative for the deflection  $w$  and continuity of the function for the shear strains. The beam is partitioned into elements, one of which is shown in Fig. 3. At each node the unknowns are the value of the deflection  $w$ , the slope  $w'$ , and the value of the

shear strains in each of the layers. For the five-layer plate of Fig. 2, five unknowns are associated with each node.

The variation of  $w$  within the element is specified as cubic, while the variation of the shear strains is taken to be linear. Both variations are thus uniquely determined by the nodal parameters,

$$w = \left(1 - 3 \frac{\xi \epsilon_2}{h^2} + 2 \frac{\xi \epsilon_3}{h^3}\right) w_i + \left(\xi - 2 \frac{\xi \epsilon_2}{h} + \frac{\xi \epsilon_3}{h^2}\right) w_i' + \left(3 \frac{\xi \epsilon_2}{h^2} - 2 \frac{\xi \epsilon_3}{h^3}\right) w_j + \left(-\frac{\xi \epsilon_2}{h} + \frac{\xi \epsilon_3}{h^2}\right) w_j' \quad (18)$$

and for the  $n$ th layer,

$$\gamma_n = \left(1 - \frac{\xi}{h}\right) \gamma_{ni} + \frac{\xi}{h} \gamma_{nj} \quad (19)$$

Using Eqs. 18 and 19, the functions in energy expression can be written as follows:

$$\begin{aligned} w'' &= \langle M_1 \rangle \cdot \delta, & \gamma_3' &= \langle M_4 \rangle \cdot \delta, \\ \gamma_1' &= \langle M_2 \rangle \cdot \delta, & \gamma_1 &= \langle M_5 \rangle \cdot \delta, \\ \gamma_2' &= \langle M_3 \rangle \cdot \delta, & \gamma_2 &= \langle M_6 \rangle \cdot \delta, \\ \gamma_3 &= \langle M_7 \rangle \cdot \delta \end{aligned} \quad (20)$$

where  $\{\delta\}$  is the vector of unknown nodal parameters

$$\{\delta\} = \begin{Bmatrix} w_i \\ w_i' \\ \gamma_{1i} \\ \gamma_{2i} \\ \gamma_{3i} \\ w_j \\ w_j' \\ \gamma_{1j} \\ \gamma_{2j} \\ \gamma_{3j} \end{Bmatrix} \quad (21)$$

and the row vectors  $\langle M_i \rangle$  are given by

$$\begin{aligned} \langle M_1 \rangle &= \left( -\frac{6}{h^2} + \frac{12\xi}{h^3}, -\frac{4}{h} + \frac{6\xi}{h^2}, 0, 0, 0, \right. \\ &\quad \left. \frac{6}{h^2} - \frac{12\xi}{h^3}, -\frac{2}{h} + \frac{6\xi}{h^2}, 0, 0, 0 \right) \\ \langle M_2 \rangle &= \left( 0, 0, -\frac{1}{h}, 0, 0, 0, 0, \frac{1}{h}, 0, 0 \right) \\ \langle M_3 \rangle &= \left( 0, 0, 0, -\frac{1}{h}, 0, 0, 0, 0, \frac{1}{h}, 0 \right) \\ \langle M_4 \rangle &= \left( 0, 0, 0, 0, -\frac{1}{h}, 0, 0, 0, 0, \frac{1}{h} \right) \\ \langle M_5 \rangle &= \left( 0, 0, 1 - \frac{\xi}{h}, 0, 0, 0, 0, \frac{\xi}{h}, 0, 0 \right) \\ \langle M_6 \rangle &= \left( 0, 0, 0, 1 - \frac{\xi}{h}, 0, 0, 0, 0, \frac{\xi}{h}, 0 \right) \\ \langle M_7 \rangle &= \left( 0, 0, 0, 0, 1 - \frac{\xi}{h}, 0, 0, 0, 0, \frac{\xi}{h} \right) \end{aligned} \quad (22)$$

The stiffness matrix  $[K]$  for the element is then a  $10 \times 10$  symmetric matrix with components  $k_{ij}$  given by

$$\begin{aligned} k_{ij} = \int_0^h \left\{ 2Q_1 M_{1i} M_{1j} + Q_2 M_{1i} M_{2j} + \right. \\ Q_2 M_{1j} M_{2i} + Q_3 M_{1i} M_{3j} + Q_3 M_{1j} M_{3i} + \\ Q_4 M_{1i} M_{4j} + Q_4 M_{1j} M_{4i} + 2Q_5 M_{2i} M_{2j} + \\ 2Q_6 M_{3i} M_{3j} + 2Q_7 M_{4i} M_{4j} + \\ Q_8 M_{2i} M_{3j} + Q_8 M_{2j} M_{3i} + Q_9 M_{2i} M_{1j} + \\ Q_9 M_{2j} M_{1i} + Q_{10} M_{3i} M_{1j} + Q_{10} M_{3j} M_{1i} + \\ 2Q_{11} M_{5i} M_{5j} + 2Q_{12} M_{6i} M_{6j} + 2Q_{13} M_{7i} M_{7j} + \\ Q_{14} M_{5i} M_{6j} + Q_{14} M_{5j} M_{6i} + Q_{15} M_{6i} M_{7j} + \\ \left. Q_{15} M_{6j} M_{7i} \right\} d\xi \quad \left( \begin{matrix} i=1,10 \\ j=1,i \end{matrix} \right) \end{aligned} \quad (23)$$

where, for example,  $M_{1i}$  is the  $i$ th component of the row vector  $\langle M_1 \rangle$ .

The components  $k_{ij}$  are easily generated by numerical integration, with a two-point Gaussian integration scheme sufficient for the integration of, at most, quadratic polynomials. The assembly of the global stiffness matrix and the solution of the resulting equations can be carried out with standard finite-element analysis techniques (Zien-

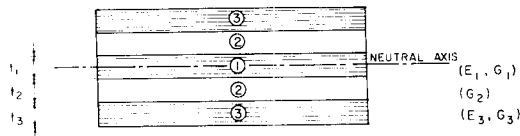


FIG. 2. Five-layer sandwich beam configuration.

kiewicz 1971). A completely similar approach can be followed for layered systems with more (or less) than the five layers considered in the particular case studied here.

APPLICATION OF THE THEORY TO PLYWOOD SHEAR DEFLECTIONS<sup>2</sup>

Consider a plywood beam with the particular lay-up of Fig. 2 and loaded on a single 12-inch span with a concentrated load at midspan. The beam width was 2 inches and the load was applied on the entire width. This case was used to study the convergence of the finite-element approach and to verify experimentally the numerical results. Two tests were made

<sup>2</sup> A computer program, based on the theoretical model presented in this paper and coded in FORTRAN IV, is available from the Western Forest Products Laboratory, Canadian Forestry Service, 6620 N.W. Marine Drive, Vancouver, B.C. V6T 1X2 Canada. The program can be used with 3,5 and 7-ply plywood. Continuous beams of up to four spans can be studied. Plywood geometric and elastic properties are entered ply by ply. Output includes the deflected shape, maximum bending, and rolling shear stresses. The program is simple to use and full input instructions are given.

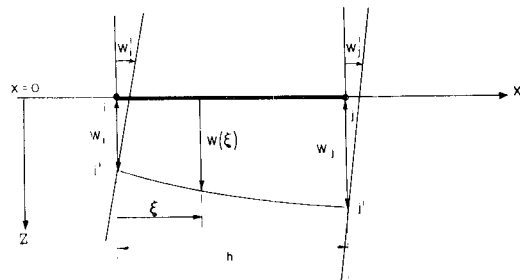


FIG. 3. Finite element—original and displaced position.

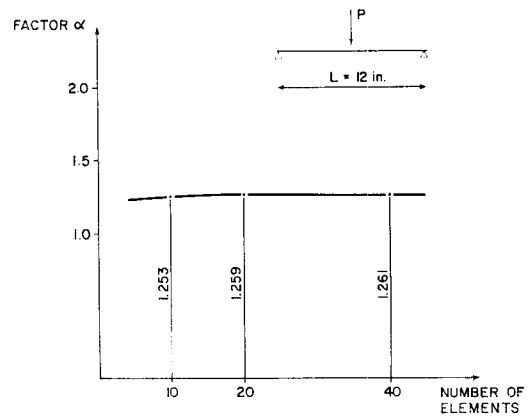


FIG. 4. Finite element analysis convergence test for factor  $\alpha$ , five-layer Test A specimen.

with the plywood soaked in water until the moisture content was about 32%. In test A, all plies were Douglas-fir [*Pseudotsuga mensiesii* (Mirb.) Franco]; in test B, Douglas-fir was used for the face plies and the center ply only, while white spruce [*Picea glauca* (Moench) Voss] was used for the cores. The individual ply thicknesses, obtained as mean of measured values over 36 specimens, are shown in Table 1.

Table 2 shows the moduli of elasticity for the soaked plies, determined experimentally with the exception of  $G_1$  and  $G_3$  ( $G_{LR}$  for Douglas-fir). The shear modulus was assumed to be related to  $G_{RT}$  of Douglas-fir according to  $G_{LR} = 10 G_{RT}$ , a relationship which approximately holds for a moisture content of 11.2% (U.S. Forest Service 1955), (Kollmann and Côté 1968). The ratio between  $G_{LR}$  and  $G_{RT}$  is assumed to remain constant for higher moisture contents. This

TABLE 1. Mean thicknesses of plies for five-layer test specimens

	Test A	Test B
N	36	36
$t_1$ (in.)	0.102	0.105
$t_2$ (in.)	0.099	0.098
$t_3$ (in.)	0.101	0.098

TABLE 2. Moduli of elasticity for five-layer test specimens

	Douglas-fir			W. spruce
	$G_2$ ( $10^3$ psi)	$G_1 = G_3^*$ ( $10^3$ psi)	$E_1 = E_3$ ( $10^6$ psi)	$G_2$ ( $10^3$ psi)
N	6	-	22	6
Mean	5.29	52.9	1.66	1.43
s	0.94	-	0.22	0.20
C.V. (%)	17.8	-	13.3	14.0
95% Conf. interval for mean	4.21 - 6.37	42.1 - 63.7	1.56 - 1.76	1.20 - 1.66

\* Based on  $G_{LR} / G_{RT} = 10$  (U.S. Forest Service, 1955).

is shown to be approximately true for Sitka spruce (Kollmann and Côté 1968). As will be shown later, the influence of the shear modulus for the face plies and center is not great and a very accurate measurement of this shear modulus is not needed.

Modulus  $G_2$  was measured using ASTM Standard Test D-2718 for plywood in rolling shear; Moduli  $E_1$  and  $E_3$  were obtained with ASTM Standard Test D-3043, Method C, for plywood in flexure under a pure moment.

In general, the maximum deflection  $\Delta$  can be expressed as the product of the maximum deflection  $\Delta_o$ , calculated by using ordinary beam bending theory times an amplification factor  $\alpha$  which accounts for the shear contribution to the deformation,

$$\Delta = \alpha \Delta_o \tag{24}$$

TABLE 3. Constant  $\beta$  for calculation of  $\Delta_o$ , maximum deflection due to bending only, using uniformly distributed load

Beam Configuration	$\beta$
	0.013021
	0.005208
	0.006770
	0.006324

In the case of a simply supported beam with a concentrated load at midspan,

$$\Delta_o = \frac{PL^3}{48EI} \tag{25}$$

and  $P$  = concentrated load  
 $L$  = span of the beam  
 $EI$  = panel stiffness

The panel stiffness  $EI$  is computed, as usual in plywood design, by neglecting the contribution of the weak cores and considering each stiff layer with its corresponding modulus  $E$ .

Using the mean values for the moduli of elasticity of Table 2 and the finite element analysis, the theoretical factor  $\alpha$  was obtained for test A for different numbers of

TABLE 4. Amplification factor  $\alpha$ . Comparison between experimental and theoretical results

	Test A	Test B
N	36	36
Mean	1.323	1.713
s	0.162	0.172
C.V. (%)	12.3	10.0
95% Conf. Interval for Mean	1.267 - 1.379	1.654 - 1.772
Theoretical Interval for Mean	1.218 - 1.329	1.707 - 1.986

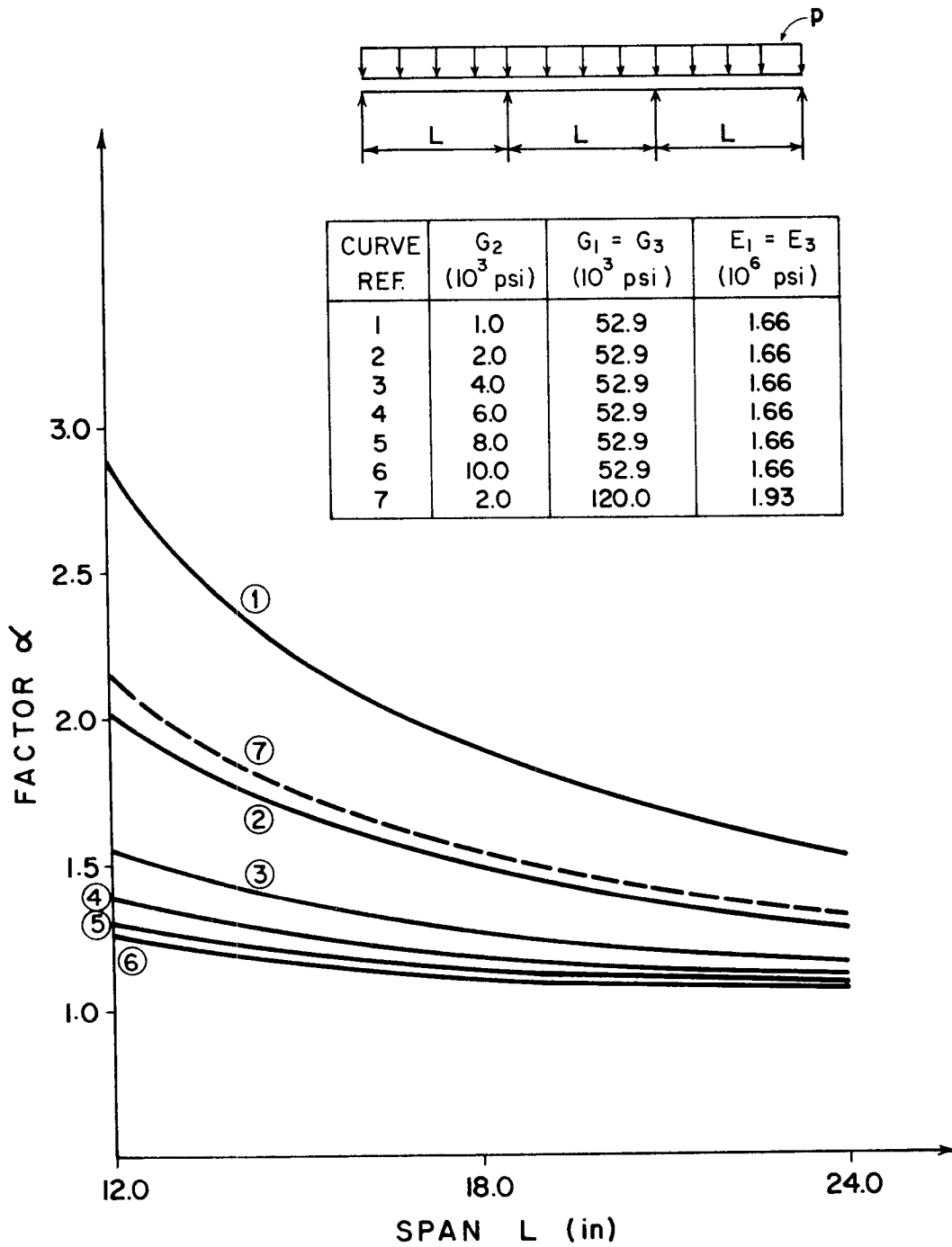


FIG. 5. Amplification factor  $\alpha$  for 3-span beam, 5-ply plywood panel, using different elastic moduli.

elements along the span. The results are shown in Fig. 4, where it is apparent that convergence is rapidly obtained with few elements.

Agreement between experimental and theoretical predictions was tested by comparison of the 95%-confidence interval for the mean factor  $\alpha$  measured from tests A and B and the theoretical interval obtained using the 95%-confidence intervals for the mean of the moduli of elasticity as given in Table 2. Theoretical and experimental intervals for the mean factor  $\alpha$  are shown in Table 4. The agreement is good, with a relatively high degree of overlapping.

In the general case of continuous beams uniformly loaded, the maximum deflection  $\Delta$  can also be expressed as in Eq. 24. The deflection  $\Delta_0$  is given, in this case, by

$$\Delta_0 = \beta \frac{pL^4}{EI} \quad (26)$$

where  $p$  = uniformly distributed load,  
 $\beta$  = constant, given in Table 3 for different beam configurations.

As a numerical example, consider the same plywood panel of tests A and B but in a three-span continuous beam configuration. The deflection  $\Delta_0$  is obtained from Eq. 26 and Table 3 and corresponds to the central deflection in the end span of the beam. Figure 5 shows the factor  $\alpha$  as a function of the span  $L$  and for several shear modulus  $G_2$  for the weak core. Other moduli were kept constant and as given, for Douglas-fir, by the mean values of Table 2. It is apparent that large shear contributions to the deflection develop as the core is made weaker in shear and that this effect is more important the shorter the span. The effect, for this lay-up, of changing the elastic and shear modulus of the stiff plies is not very significant, as shown by comparison of curves 7 and 2 of Fig. 5. The cores can be made weaker in shear by either making them thicker or by

using a weaker species like white spruce, two situations that should be considered in designing lay-ups for use under high moisture-content conditions.

#### CONCLUSIONS

A finite-element approach to the problem of deflection of multi-layered sandwich beams or plates with layers weak in shear has been developed. The numerical method was applied to the case of plywood panels and shown to converge well, with few elements needed for reliable results. Theoretical predictions agree well with experimental measurements in the sense that confidence intervals for the maximum deflection measured in experiments can be estimated by using the theoretical approach and taking into account the corresponding confidence intervals for the elastic moduli. The influence of weaker cores in the deflection of plywood panels, through shear deformation, has been shown to be significant and should be taken into account in design criteria.

#### REFERENCES

- AZAR, J. J. 1968. Bending theory for multilayer orthotropic sandwich plates. *AIAA J.* 6(11): 2166-2169.
- CHIU, Y. M., AND E. BIBLIS. 1971. An analysis of flexural rigidity of 7-ply southern pine plywood strips at short spans parallel to face grain. *Wood Fiber* 3(2):112-120.
- KIATUA, T. P., AND Y. K. CHEUNG. 1972. Triangular element for multilayer sandwich plates. *J. Eng. Mech. Div. ASCE* 98(EM5): 1225-1238.
- KOLLMANN, F. F. P., AND W. A. CÔTÉ. 1968. Principles of wood science and technology, v. I. Springer-Verlag, N.Y., pp. 294 and 309.
- PLANTEMA, F. J. 1966. Sandwich construction. John Wiley, New York.
- U.S. FOREST SERVICE. 1955. Wood handbook. U.S. Dep. Agr. Handbook No. 72, Washington, D.C. p. 79.
- ZIENKIEWICZ, O. C. 1971. The finite element method in engineering science. McGraw-Hill, London.

APPENDIX I—CONSTANTS  $Q_i$ 

Let  $e_n = (z_n + z_{n+1})/2$ , then

$$Q_1 = \frac{E_1 t_1^3}{24} + \frac{E_3 t_3^3}{12} + E_3 t_3 e_3^2;$$

$$Q_2 = -E_1 \frac{t_1^3}{16} - \frac{2}{3} E_3 e_3 t_1 t_3;$$

$$Q_3 = -E_1 \left( \frac{G_2}{G_1} \right) \frac{t_1^3}{60} - 2E_3 t_3 e_3 \left( t_2 + \frac{G_2}{G_1} \frac{t_1}{6} \right) - \frac{E_3}{3} \frac{G_2}{G_3} t_3^2 \left( e_3 + \frac{t_3}{20} \right);$$

$$Q_4 = -\frac{2}{3} E_3 t_3^2 \left( e_3 + \frac{t_3}{5} \right);$$

$$Q_5 = \frac{51}{1890} E_1 t_1^3 + \frac{E_3}{9} t_3 t_1^2;$$

$$Q_6 = \frac{E_1}{504} \left( \frac{G_2}{G_1} \right)^2 t_1^3 + \frac{19}{630} \left( \frac{G_2}{G_3} \right)^2 E_3 t_3^3 + E_3 t_3 \left( \frac{G_2}{G_1} \frac{t_1}{6} + t_2 \right) \left( \frac{G_2}{G_1} \frac{t_1}{6} + t_2 + \frac{G_2}{G_3} \frac{t_3}{3} \right);$$

$$Q_7 = \frac{52}{315} E_3 t_3^3;$$

$$Q_8 = \frac{4}{315} E_1 \left( \frac{G_2}{G_1} \right) t_1^3 + \frac{2}{3} E_3 t_1 t_3 \left( \frac{G_2}{G_1} \frac{t_1}{6} + t_2 \right) + \frac{E_3}{9} t_1 t_3^2 \left( \frac{G_2}{G_3} \right);$$

$$Q_9 = \frac{2}{9} E_3 t_1 t_3^2;$$

$$Q_{10} = \frac{2}{3} E_3 t_3^2 \left( \frac{G_2}{G_1} \frac{t_1}{6} + t_2 \right) + \frac{13}{105} E_3 t_3^3 \left( \frac{G_2}{G_3} \right);$$

$$Q_{11} = \frac{4}{15} G_1 t_1;$$

$$Q_{12} = \frac{G_1 t_1}{10} \left( \frac{G_2}{G_1} \right)^2 + G_2 t_2 + \frac{2}{15} \left( \frac{G_2}{G_3} \right)^2 G_3 t_3;$$

$$Q_{13} = \frac{8}{15} G_3 t_3;$$

$$Q_{14} = \frac{2}{15} G_2 t_1;$$

$$Q_{15} = \frac{2}{15} G_2 t_3.$$